Image Analysis of the AXAF VETA-1 X-ray Mirror

M. Freeman, J. Hughes, L. Van Speybroeck

Smithsonian Astrophysical Observatory
60 Garden St.
Cambridge, MA 02138
(617)495-7000

J. Bilbro, M. Weisskopf

Space Sciences Laboratory
NASA / George C. Marshall Space Flight Center
ES 65, Huntsville, Alabama 35812
Phone (205)544-5498 FAX (205)544-7754

ABSTRACT

Initial core scan data of the VETA-1 x-ray mirror proved disappointing, showing considerable unpredicted image structure and poor measured FWHM. 2-D core scans were performed, providing important insight into the nature of the distortion. Image deconvolutions using a raytraced model PSF was performed successfully to reinforce our conclusion regarding the origin of the astigmatism. A mechanical correction was made to the optical structure, and the mirror was tested successfully (FWHM 0.22 arcsec) as a result.

1. INTRODUCTION

The Verification Engineering Test Article - 1 (VETA-1) was a subset of the High Resolution Mirror Assembly (HRMA), the AXAF flight optics. It consisted of the outer mirror pair (P1/H1) in the polished but uncut and uncoated state. The goal of the VETA-1 test was to demonstrate the feasability of polishing grazing incidence x-ray optics to the level required by the stated AXAF mission requirements. The Congressionally-mandated milestone was a FWHM of 0.5 arcsec for the optic, to be reported by mid-September. The VETA-1 and its associated test hardware were placed in the X-ray Calibration Facility (XRCF) at NASA's Marshall Space Flight Center (MSFC) during the last weeks of August, 1991. Pumpdown of the chamber began on the evening of Friday, Aug. 30. It was found that 2-3 days were required to achieve thermal stabilization at vacuum before running critical tests. Using the VETA X-ray Detection System (VXDS) and a quadrant shutter placed behind the mirror, relative alignment of the opical elements was performed, first using the VXDS imaging detector, and then the VXDS proportional counters and apertures. By Monday, Sept. 2, the alignment and focus adjustments were complete, and we began detailed pinhole scan measurements of the VETA-I image.

Initial one-dimensional (1-D) core scans through the image center at the best RMS focus showed a marked bimodal shape in the intensity distribution (Fig. 1). Even after many 1-D scans, the unexpected shape and large variation of measured FWHM with scan position and direction did not yield the needed understanding of the image, instead indicating significant two-dimensional (2-D) structure. In addition, the measured FWHM was not sufficiently better than 0.5 arcsec to avoid concerns of measurement

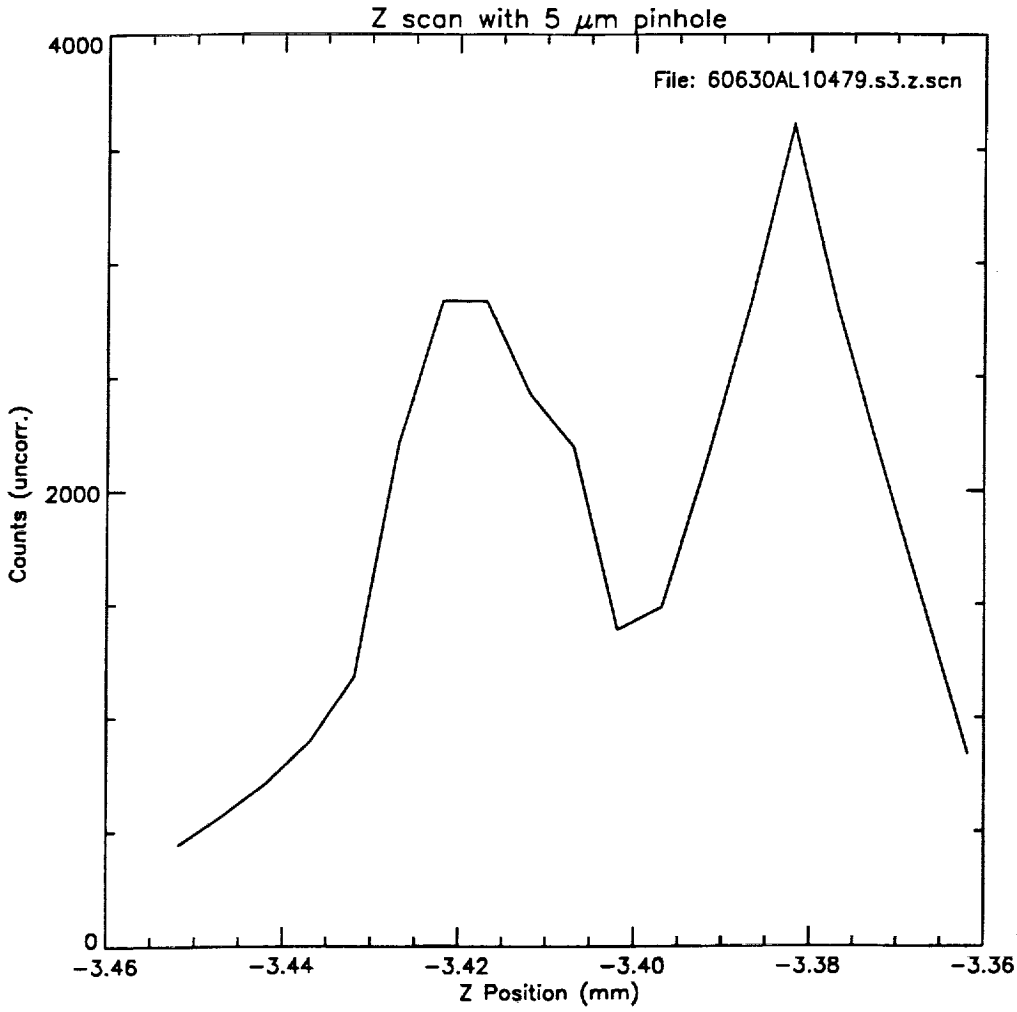

Figure 1. One-Dimensional Core Scan (Sept. 2, 1991)

error. It was determined that to provide a better understanding of the image, it was necessary to perform a 2-D raster scan of the entire image core. Weighing image detail against test time, a 19 by 19 raster pattern using the 10 μm pinhole was chosen, producing a sampled image of the inner 4 arcsec core of the point response function (PRF).

2. INITIAL 2-D CORE SCANS

The first complete 2-D scan (ID: 10579) of the image, taken 6 days into the test (Sept. 5), is shown in Fig. 2, in (a) as an isometric intensity plot, and (b) as isointensity contours. This pattern of isometric view followed by contours will be used throughout for image display. The 19 by 19 data were resampled in the following images by 4 in each axis for visualization. An aluminum anode target, which produces characteristic line radiation at approximately 1.488 keV, and the flow proportional counter (FPC) were used. Note that the intensity corresponds the the number of counts accumulated from the FPC spectra in an operator defined region-of-interest (ROI). No corrections were made for deadtime, since the deadtime was dominated by the Beam Normalization Detector (BND) count rate, making the *relative* deadtime correction over the image only of order a few percent. Pulse pile-up

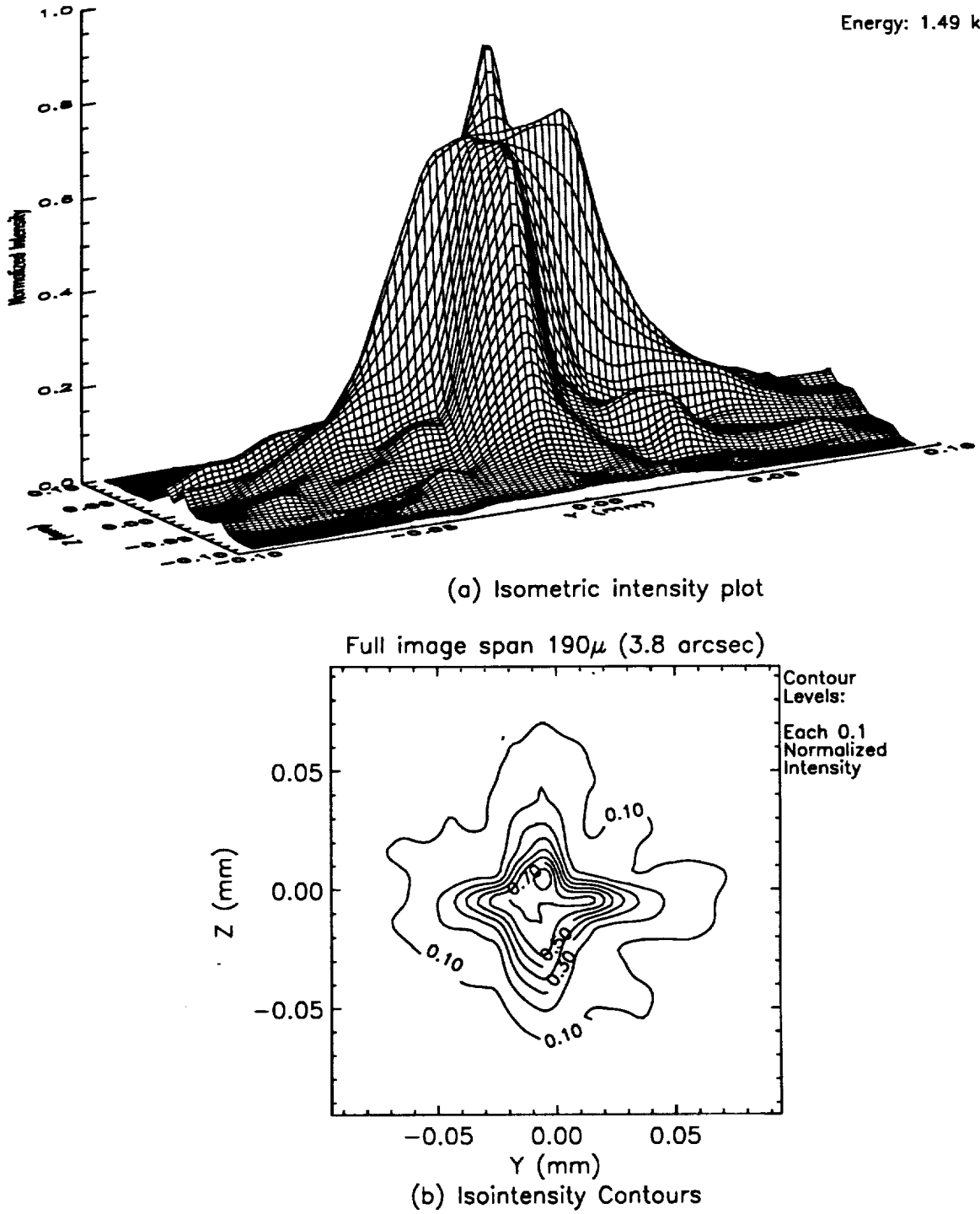

Figure 2. 19 x 19 Scan with 0.010 mm Pinhole
File: 1000AL10579.scn

SAO/VXDS 31Jul92

corrections were also ignored for these analyses, but are expected to be of order a few percent, since the source intensity was controlled to limit the maximum count rate.

The image showed a significant "cross" structure. The alignment of the cross with the gravity vector provided an indication of the origin of the distortion (the y-axis of the images shown [labelled Z] is the anti-gravity direction). Although it was known that gravity produced ovalization of the optics, no raytrace predictions of the most recent Kodak finite element model of the optics in the test configuration had been performed by SAO. Work began immediately to perform these analyses. In addition, we compared the focal position measured using only the top and bottom mirror quadrants to that of only the left and right, and found them to differ by approximately 600 μm.

3. MODEL POINT SPREAD FUNCTION

A NASTRAN Finite Element Analysis (FEA) model of the VETA-I in the test configuration was obtained by SAO from Eastman Kodak, the load in this case being the body forces due to gravity. The resultant predicted distortion, after removal of the rigid body effects, was primarily ovalization with a magnitude of 4.95 μm (zero to peak) for the paraboloid (P1) and 3.43 μm for the hyperboloid. SAO produced an independent ANSYS model, with predicted values within 20% of the EKC model. Using SAO-developed software and OSAC, a raytrace code developed by Perkin-Elmer (P. Glenn et. al.), the FEA model data was fit with Legendre-Fourier polynomials and raytraced. Included in the raytrace model and the subsequent post-processing were the following effects:

1. Finite Source Distance (518.16 m)
2. Finite Source Size (.22 arcsec dia.)
3. P1-H1 Despace (109.03 mm)
4. Calculated Gravitational Distortion (above)
5. Zerodur Reflectivity at 1.488 keV
6. ΔΔR errors (RMS = 0.098 arcsec, from HDOS)
7. Circumfrential slope errors: 6.446 μrad (P1) and 9.745 μrad (H1)
8. Sag errors: 1585 Å (P1) and 447 Å (H1)
9. Axial slope errors:
    a. Low frequency gaussian core: 0.158 arcsec
    b. Mid-frequency PSD term: 25 Å (18 mm correlation length)
    c. Upper Mid-frequency PSD term: 10 Å (0.35 mm correlation length)
    d. High frequency PSD term: 7 Å (0.018 mm correlation length)

The first four will be referred to as 'Facility Effects': Inclusion of just these terms is equivalent to assuming a perfect mirror in the test configuration. No residual misalignment of P1 to the X-ray Calibration Facility (XRCF) or P1 to H1 was assumed. Excellent relative positional stability of the source, optics, and detectors was realized based on inspection of the Motion Detection System (MDS) data. For this reason, we decided to ignore the effects of vibration in the simulation. Finally, the focal plane ray file was sampled to simulate the actual 10 circular pinhole scan.

The results are shown in Fig. 3 (a) and (b), exhibiting good qualitative agreement with the measured image. An algorithm was created to perform a simple image subtraction by scaling the simulation to the peak of the measured image, then aligning them for minimum RMS difference. This resulted in an RMS residual of 3.7%, a peak residual of 33.5%, and a correlation coefficient of 0.961. These data and the measured focus difference pointed more strongly to the 1g ovalization as the source of the image distortion, although work continued to determine if there were reasonable alternate hypotheses. At this point, engineering personnel from the Eastman Kodak Co. (EKC), the designers of the mirror support structure, began to consider possible ways to correct the problem. SAO, TRW and MSFC staff desired even more concrete evidence that this was indeed the cause, since the solution would most likely involve breaking vacuum, making mechanical changes to the VETA-1 assembly, and another pumpdown. With only days left before the FWHM needed to be reported, such a significant loss of test time could only be contemplated if the confidence that it would correct the problem was *very* high.

4. DECONVOLUTION AND SUPPORTING DATA

Given that the fit to of the model to the data was reasonable, deconvolution of the facility effects from the raw data was attempted. The assumption was made that the superposition of the facility effects (F), such as the gravitational distortion or the finite source distance (see above), and the "true" imaging performance of P1/H1 (P) could be represented as a two-dimensional convolution to yield the test data (D):

$$D = F \otimes P \equiv \int_{-\infty}^{\infty} F(R-r)P(r)dr.$$

The ultimate aim of the restoration was to restore the 'true' imaging performance of P1/H1, ie. remove the 'facility effects'.

The general approach entailed resampling the 10 μm pinhole 19x19 point raster scan image onto 1 μm × 1 μm pixels, to yield D. The convolution kernel F was defined by running a raytrace of a perfect mirror (i.e., without ΔΔR, circumferential slope, sag, or axial slope errors) in the test configuration, including only the facility effects as enumerated above. This was output as a FITS image with 1 μm × 1 μm pixels. This image is shown in Figure 4. Two standard techniques for deconvolution were then used: Wiener filter deconvolution and a nonlinear recursive restoration scheme described by Richardson and for astronomical use by Lucy[1][2]. Note that both of these deconvolution techniques are available under IRAF (package: stsdas.playpen). The Richardson-Lucy (R-L) technique has been heavily employed for deconvolution of HST images[3].

Wiener filter deconvolution is a simple Fourier quotient technique which uses estimates of the noise and signal power spectrum (PS) to obtain an optimally-filtered result. In our application the noise PS was assumed to be white and was computed from the input image. The PS of the convolution kernel F was assumed to be noiseless, which is only approximately correct since the raytrace which produced this function used a finite number of rays. A low pass filter (4 pixel sigma) was applied in the frequency domain. The results are shown in Figure 5. The technique restores a point image with a full width half maximum (FWHM) of 0.24 arcsec. However there is a significant amount of "ringing" in the image, which appears as ripples in the zero level. This is often the case with this type of deconvolution technique and arises because of the sharp digital filter and the lack of a constraint requiring the restoration of positive counts only.

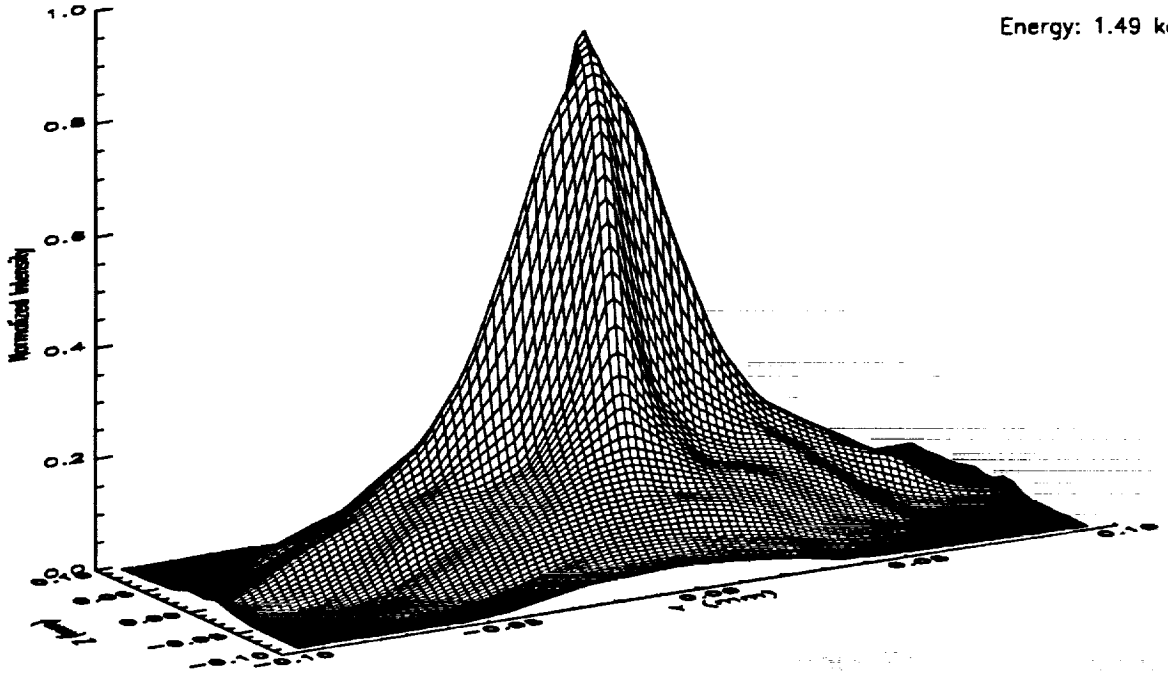

(a) Isometric intensity plot

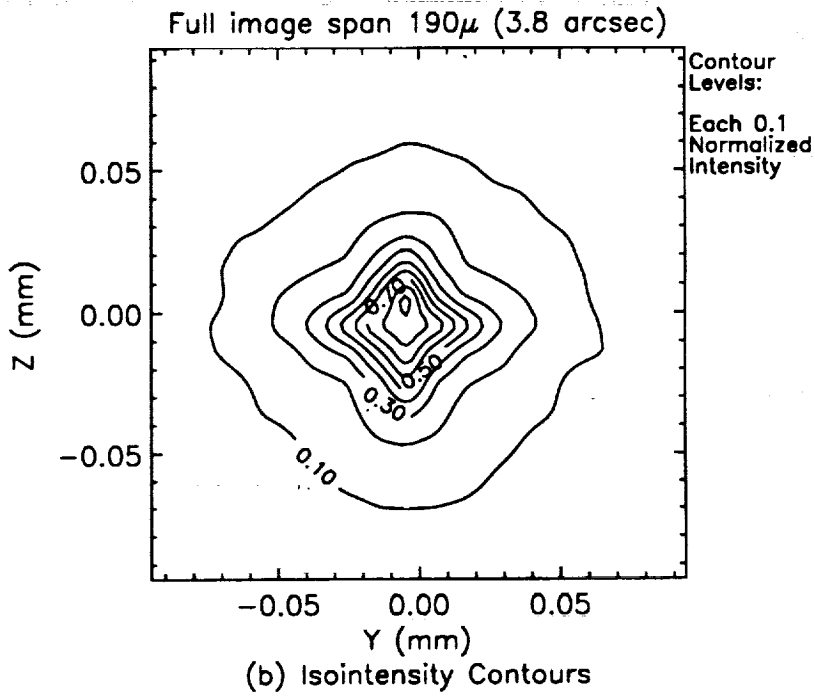

(b) Isointensity Contours

Figure 3. SAO Raytrace Prediction of VETA–I Performance
EKC Structural Model of 1g Deformation

SAO/VXDS 31Jul92

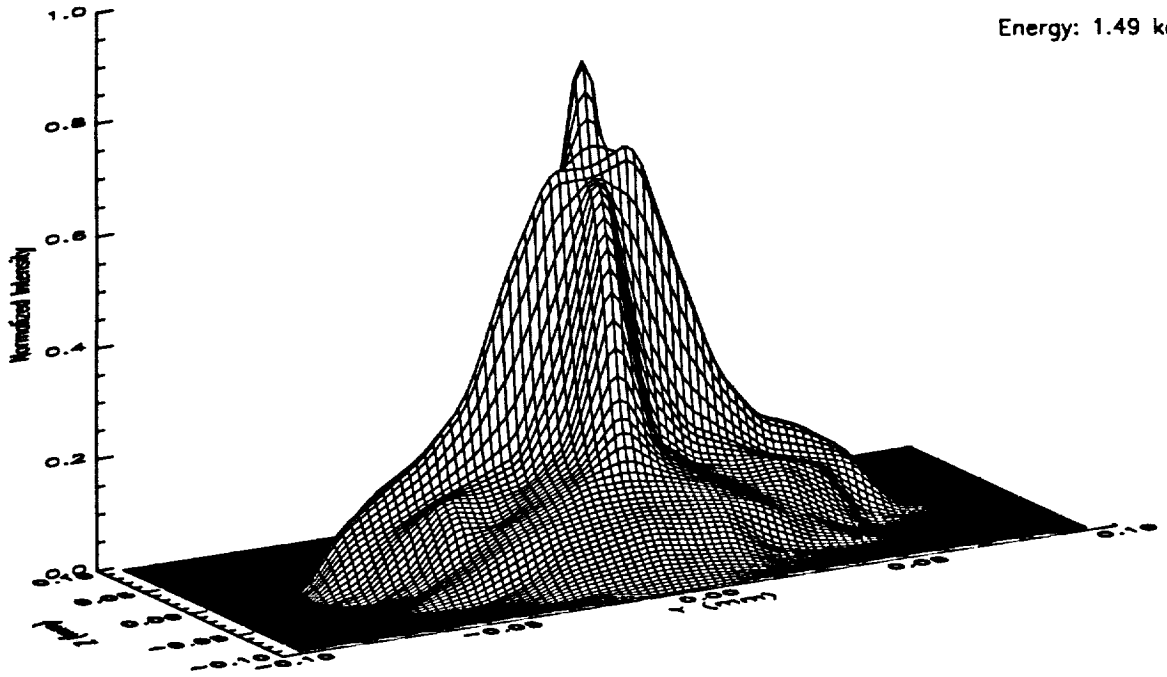

(a) Isometric intensity plot

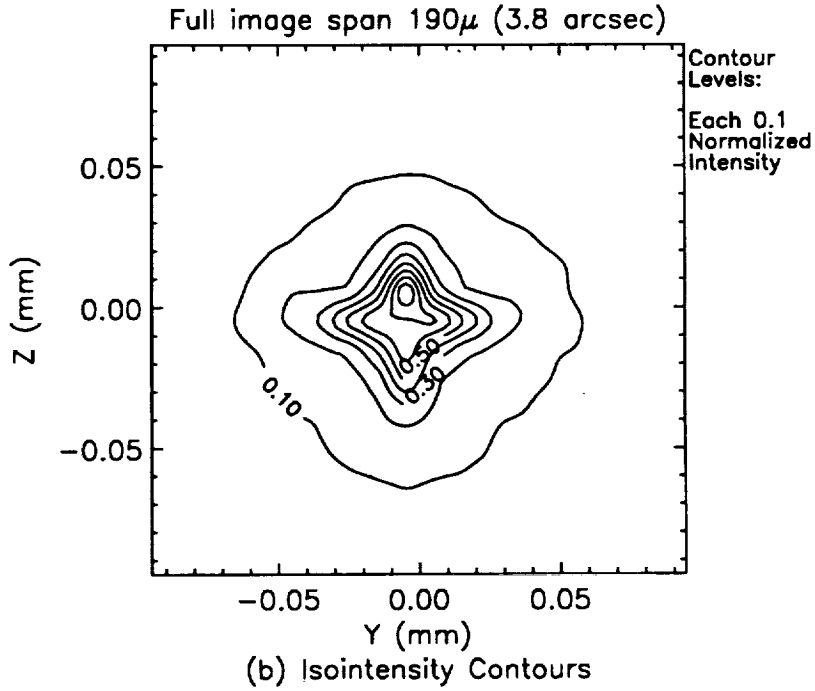

(b) Isointensity Contours

Figure 4. Facility Effects PSF
(Gravity(EKC), Finite Source Size & Distance, and Despace)

SAO/VXDS 31Jul92

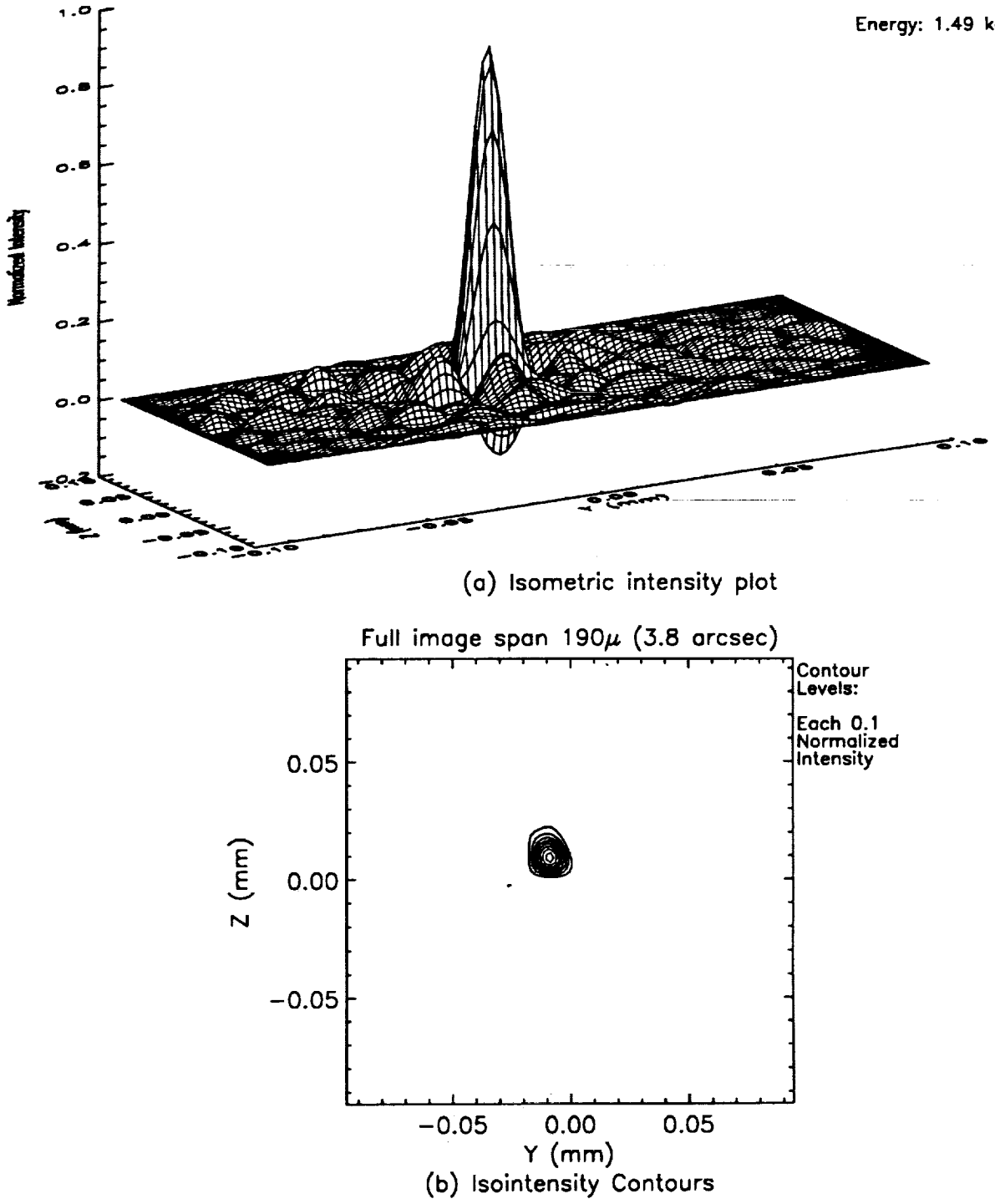

Figure 5. Wiener Deconvolution of 19x19 Scan 10579 using Facility Effects PSF

SAO/VXDS 31Jul92

The R-L image deconvolution requires that the restored data be non-negative everywhere. Furthermore it insists on *statistical* agreement between the observed data and the rectified estimate, instead of *exact* agreement and employs χ^2 as the figure of merit. One well-known shortcoming of this approach is the lack of a built-in stopping rule. We found that during the first 10 or so iterations the change in χ^2 was rapid, while after about 50 standard iterations the change in χ^2 from iteration to iteration became very small. During the test period, we used this to indicate convergence. Figure 6 shows the restored image from this technique after 8 accelerated (equivalent to ~ 50 standard) iterations. The FWHM of the imaged point source is 0.21 arcsec.

5. MIRROR GRAVITY OVALIZATION CORRECTION AND RESULTS

All indications were that we had a correct hypothesis for the source of the image distortions. EKC had determined that a force could be applied to the mirror support rings which would correct the majority of the ovalization and related distortion. The data and a correction plan were presented to appropriate project management personnel on Monday, Sept. 9. Approval was given to implement the correction, and repressurization was begun as soon as the necessary hardware had been fabricated by EKC. After the required 3 days of stabilzation, realignment of the optics began on Sept. 15. Two days later, on Sept. 17, the first 19 x 19 scan after the 1g correction had been applied was performed. The results are plotted in Figure 7, showing a much improved PRF. Later that same day we measured the FWHM with 1D scans using the 5μm pinhole to be 0.22 arcsec, the figure reported to the Congress and announced publicly.

The corresponding OSAC raytrace model PSF of the new facitity effects is shown in Figure 8. Using the same R-L deconvolution technique, we obtained the deconvolved image (after 8 accelerated iterations) shown in Figure 9.

6. DISCUSSION OF THE R-L DECONVOLUTION RESULTS

It was noted during the test work, and in subsequent processing of test images, that the Richardson-Lucy algorithm would produce continuous improvement in the estimated mirror performance for many iterations, albeit at a decreasing rate. Although the deconvolution work during the test was used primarily to establish correlation between the measured image and a model, it would be desirable to develop a "stopping rule" such that an estimate of the true mirror performance (ie. removing the facilty effects) might be made.

To investigate more completely the behavior of the restoration as a function of the number of iterations, we employed the Accelerated R-L algorithm[4] in an IDL/PV-WAVE™ implementation available from the ST-ECF. In our application, we saw an improvement in convergence rate of 5-8 over the standard R-L algorithm. This allowed us to quickly "push" the restoration to the equivalent of hundreds of standard iterations. Figure 10 shows the the FWHM plotted for both the pre- and post-correction restorations, as well as the measured value and that produced by the Wiener filter. As noted, the restoration continued to improve the image well beyond the measured value, although no direct comparison can be made since the measured FWHM includes all facility effects, most significant in this case being the source size effect. Although not evident in the restorations shown at 8 iterations, the effects of 'over-restoring' the image can be seen in Figure 11, the restoration of scan 20057 after 32 accelerated R-L iterations. Here the data variations in the outer regions of the image are beginning to be restored as separate "sources". This is inconsistent with our physical situation, and emphasizes the importance of exercising caution in the use of this technique.

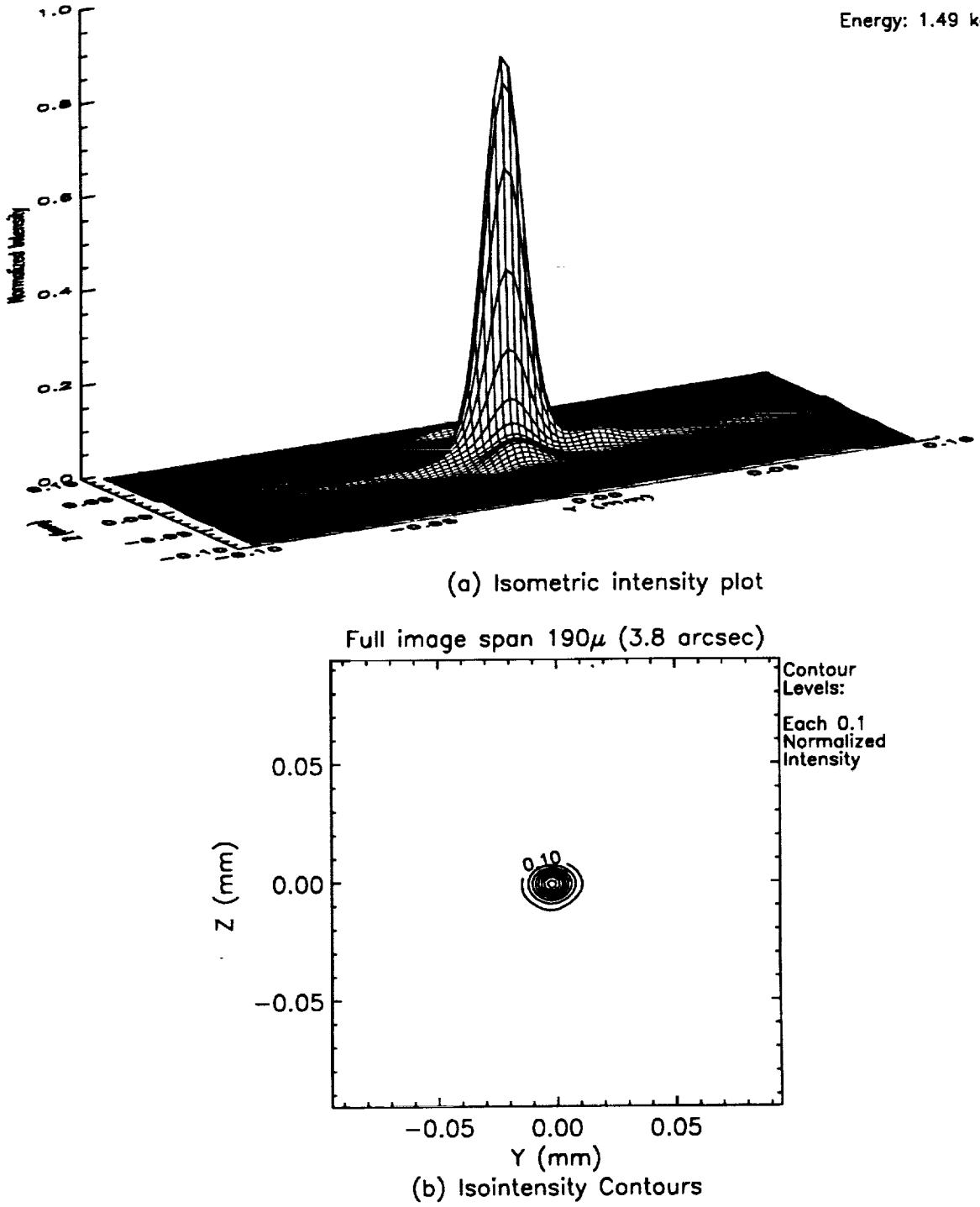

Figure 6. R−L (accel) Deconvolution of 19x19 Scan 10579 using Facility Effects PSF (8 iterations)

SAO/VXDS 31Jul92

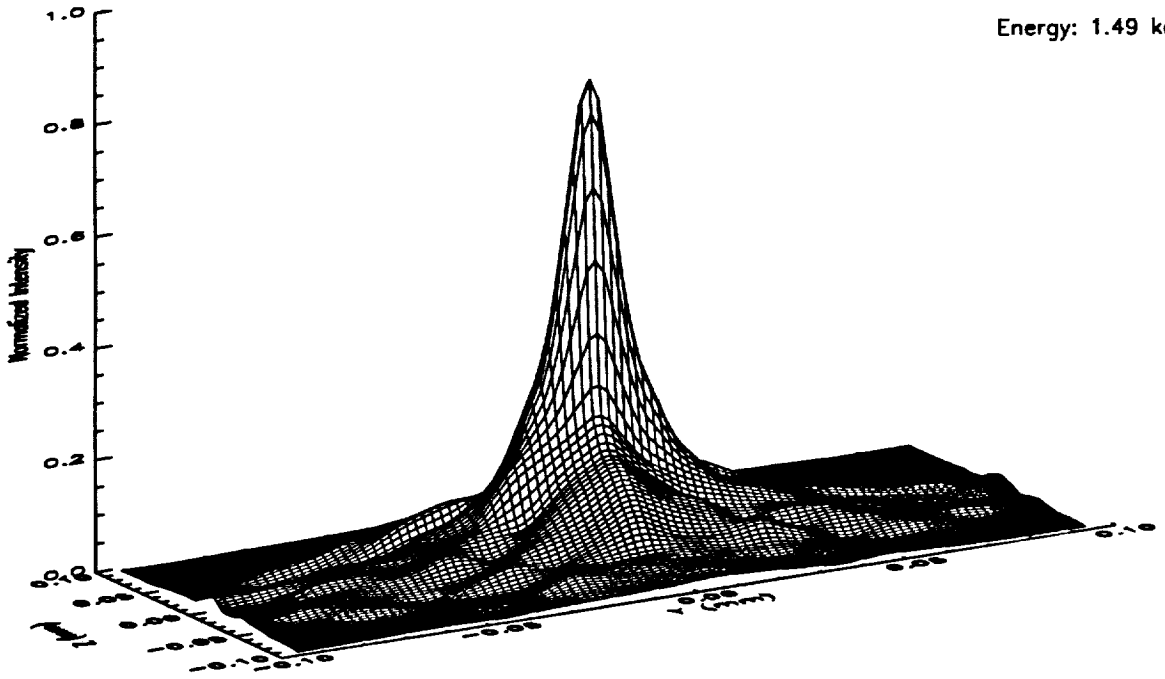

(a) Isometric intensity plot

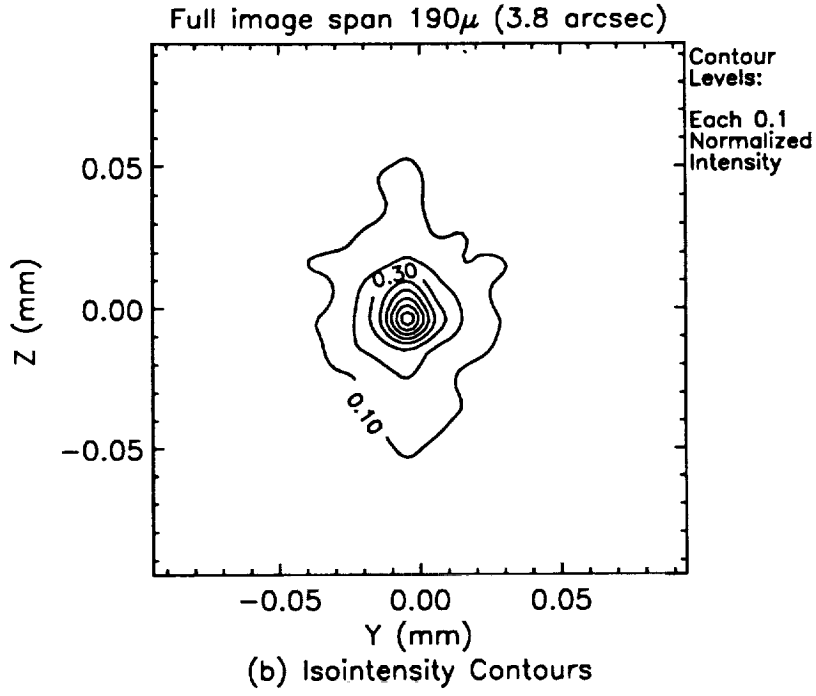

(b) Isointensity Contours

Figure 7. 19 x 19 Scan with 0.010 mm Pinhole
File: 002AL20057.scn

SAO/VXDS 31Jul92

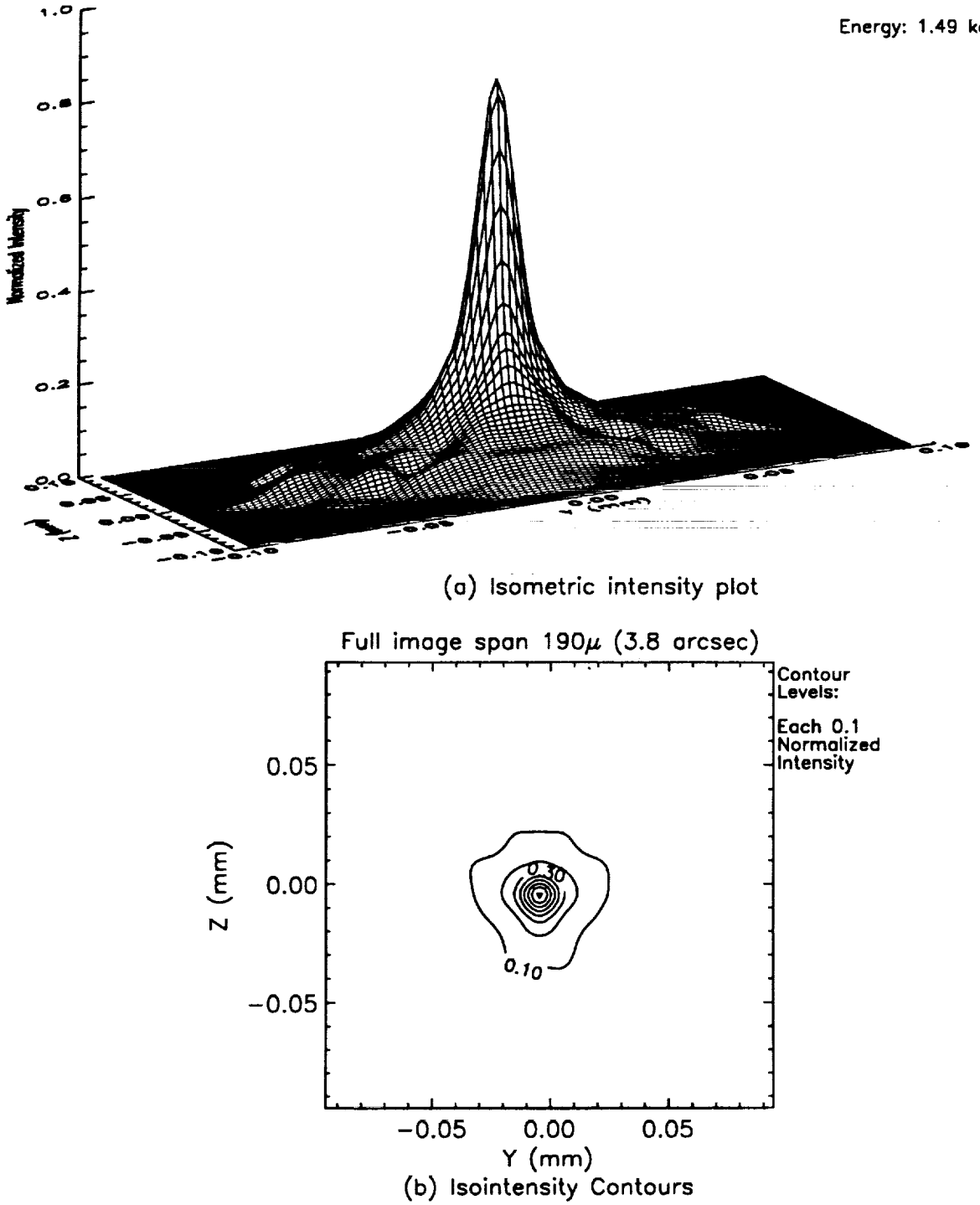

(a) Isometric intensity plot

Full image span 190μ (3.8 arcsec)

(b) Isointensity Contours

Figure 8. Facility Effects PSF with Modeled 1g Correction (Gravity(EKC), Finite Source Size & Distance, and Despace)

SAO/VXDS 31Jul92

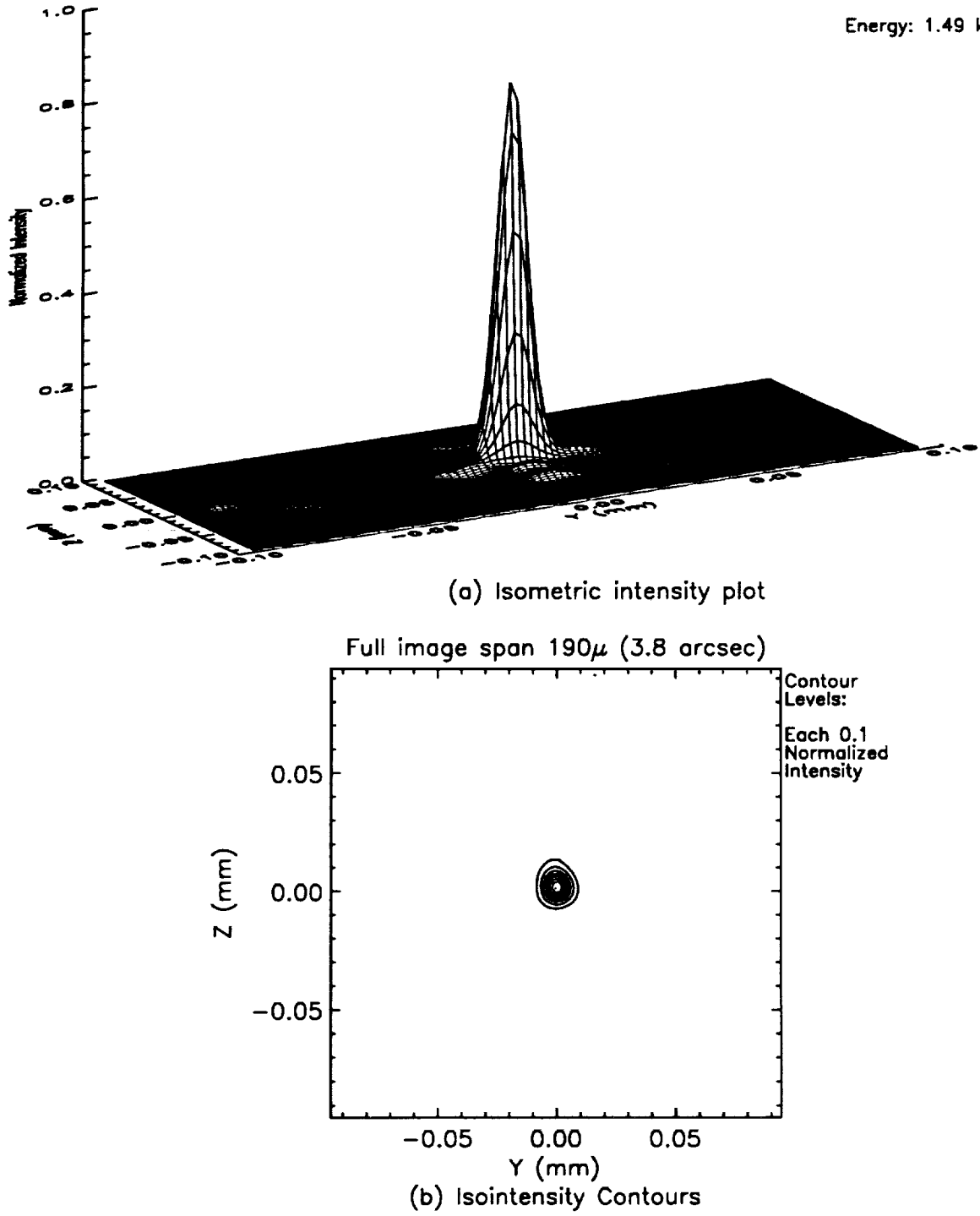

Figure 9. R–L (accel) Deconvolution of 19x19 Scan 20057 using Facility Effects PSF (8 iterations)

SAO/VXDS 31Jul92

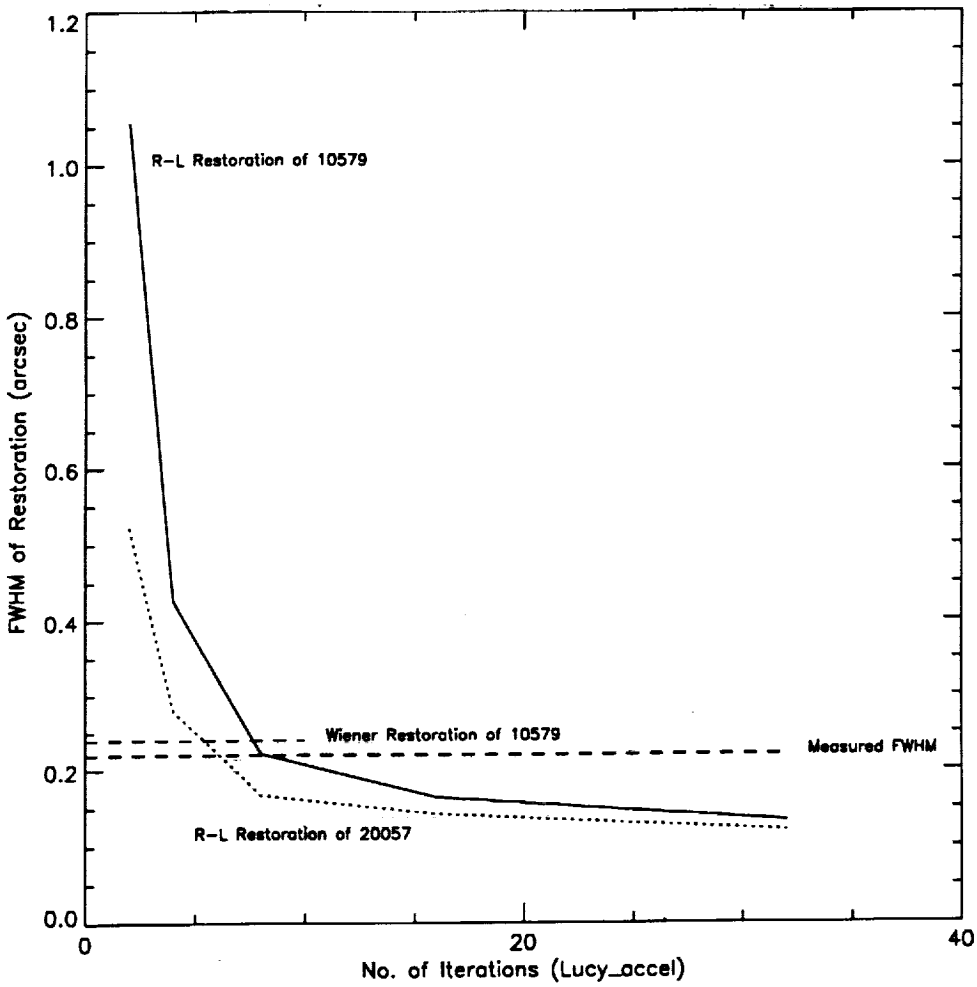

Figure 10. FWHM of Image during Restoration

7. CONCLUSIONS AND FUTURE WORK

The measurement of the VETA-1 FWHM within specification and on time was accomplished through hard work by the test and analysis personnel of SAO, TRW, Eastman Kodak, and MSFC. The information necessary to make the important real-time correction to the optic was derived in large part from analysis work, especially the R-L deconvolution, performed in parallel with the test. We believe this method of application, where certain known ofr modeled effects are deconvolved from measured data to produce a more useful representation of the system performance, is applicable to many measurement problems.

More work is necessary in the development of a R-L "stopping rule" for this application. We intend to pursue investigations of image frequency content and the statistics related to the knowledge of the model PSF as possible avenues for the development of such a rule. This work will be an important part of providing definition for the test of the HRMA.

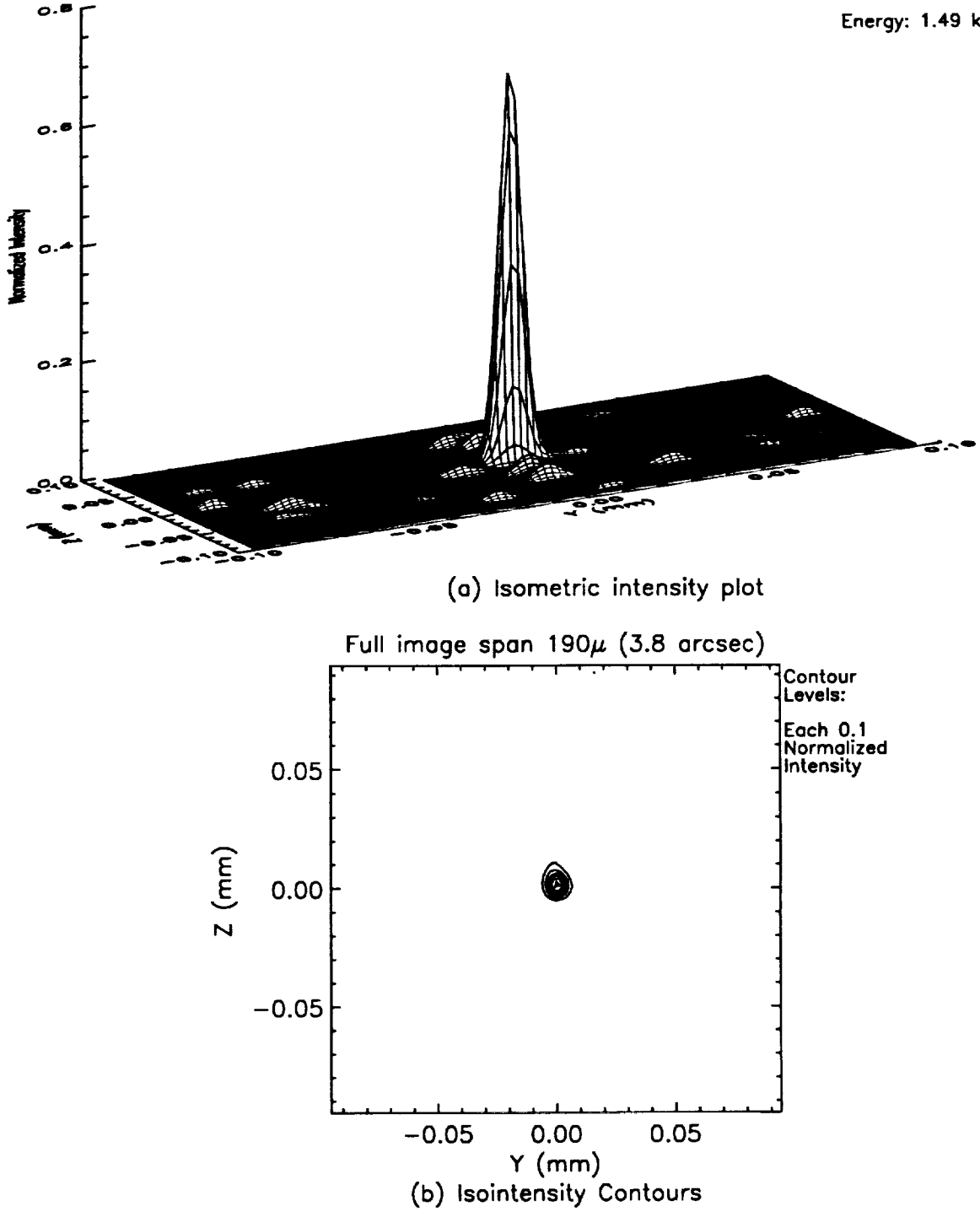

Figure 11. R–L (accel) Deconvolution of 19x19 Scan 20057 using Facility Effects PSF (32 iterations)

SAO/VXDS 31Jul92

ACKNOWLEDGEMENTS

We are grateful to H.-M. Adorf of the ST-ECF for providing the new implementation of the accelerated R-L algorithm, a useful interpolation scheme for supsampling images, and many helpful suggestions related to the application of the R-L technique.

REFERENCES

3. B. H. Richardson, J. Opt. Soc. America **62**, 55, 1972.

3. L. B. Lucy, "An iterative technique for the rectification of observed distributions", Astron. J. **79-6**, 745-754, June 1974.

3. H.-M. Adorf, J. R. Walsh, and R. N. Hook, "Restoration Experiments at the ST-ECF", **Proc. Workshop The Restoration of HST Images and Spectra**, R. L. White and R. J. Allen (eds.), Space Telescope Science Institute, Baltimore MD, 21-22 Aug. 1990.

4. H.-M. Adorf, J. R. Walsh, R. N. Hook, and F. D. Murtaugh, "Accelerating the Richardson-Lucy Algorithm", 1992 (unpublished).